

Electronic Supplementary Information

A thiolate-bridged ruthenium-molybdenum complex featuring terminal nitrido and bridging amido ligands derived from N–H and N–N bond cleavage of hydrazine

Yahui Li,^a Linan Su,^{*a} Dawei Yang,^a Kai Di,^a Baomin Wang^a and Jingping Qu^a

^aState Key Laboratory of Fine Chemicals, Dalian University of Technology, Dalian 116024, P. R. China.

*Email: lnsu@dlut.edu.cn.

Contents:

Experimental Section.....	S3
X-ray Crystallographic Information	S8
ESI High Resolution Mass Spectra	S16
NMR Spectra	S17
IR Spectra	S22

Experimental Section

General procedures

All manipulations were routinely carried out under an argon atmosphere, using standard Schlenk-line techniques. All solvents were purified by PureSolv MD5 (USA) or MB SPS-800 (Germany) solvent purification system. Deuterated solvents for NMR spectroscopy were stored over 4 Å molecular sieves under an argon atmosphere. Complex $[\text{Cp}^*\text{MoBr}_4]$ ($\text{Cp}^* = \eta^5\text{-C}_5\text{Me}_5$),¹ $[\text{Cp}^*\text{Ru}(\text{MeCN})_3][\text{PF}_6]$,² benzene-1,2-dithiol (bdtH_2),³ 2,4,6-tri-*tert*-butylphenoxy radical ($t\text{Bu}_3\text{ArO}^\cdot$)⁴ and Lut HBPh_4 ⁵ were prepared according to the literatures. $^{15}\text{N}_2\text{H}_4$ was prepared by Soxhelt extraction of $^{15}\text{N}_2\text{H}_4 \cdot \text{H}_2\text{SO}_4$ (Cambridge Isotope Laboratories) with liquid ammonia and the excess pressure derived from liquid ammonia is released through a mercury bubbler.⁶ $n\text{BuLi}$ (Aldrich), cobaltocene (CoCp_2 , Aldrich), hydrazine (Aldrich) were used as received without further purification. ***DANGER: anhydrous hydrazine can be explosive at high temperatures and should be handled with extreme caution.***

Spectroscopic measurements

The ^1H NMR spectra were recorded on a Bruker 400 Ultra Shield spectrometer. The ^{15}N NMR spectra were recorded on a Bruker Ascend 600 spectrometer. The chemical shifts (δ) are given in parts per million CD_2Cl_2 (5.32 ppm for ^1H). ^{15}N chemical shifts are referenced to external ^{15}N -nitrobenzene ($\delta = 370.4$ ppm relative to liquid ammonia at 0 ppm). Infrared spectra were recorded using a NEXVS FT-IR spectrometer. Elemental analyses were performed on a Vario EL analyzer. ESI-HRMS analyses were recorded on a UPLC/Q-Tof micro spectrometer.

X-ray crystallography procedures

The data were obtained on a Bruker SMART APEX CCD diffractometer with graphite-monochromated Mo $K\alpha$ radiation ($\lambda = 0.71073$ Å). Empirical absorption corrections were performed using the SADABS program.⁷ All of the structures were solved with the Superflip structure solution program using Charge flipping and refined with the XL refinement package using Least Squares minimization that was implanted in Olex2.⁷⁻⁹ All of the non-hydrogen atoms were refined anisotropically. All of the hydrogen atoms were generated and refined in ideal positions.

Preparation of [Cp*Mo(bdt)Br₂] (1)

A solution of bdtLi₂ in THF, prepared by the reaction of *n*BuLi (4 mL, 2.5 M in *n*-hexane, 10 mmol) and benzene-1,2-dithiol (710 mg, 5 mmol), was added dropwise to the suspension of [Cp*MoBr₄] (2.74 g, 5 mmol) at room temperature. The reaction mixture was allowed to be stirred for another 12 h. The resulting solution was evaporated to dryness under vacuum, then the residues were washed with Et₂O (3 × 20 mL) and dried in reduced pressure to obtain a brownish purple powder. Additional 50 mL of CH₂Cl₂ was used to extract the product from the residue. Evaporation of the volatiles afforded complex [Cp*Mo(bdt)Br₂] (**1**, 1.56 g, 2.94 mmol, 59%) as a brownish purple powder. Crystals of **1** suitable for X-ray diffraction experiment were grown from saturated CH₂Cl₂ solution layered by *n*-hexane at room temperature. ¹H NMR (400 MHz, CD₂Cl₂, ppm, 298 K): δ 2.21 (br). μ_{eff} (CD₂Cl₂, Evans' method, 298 K): 1.84 μ_{B} . IR (Film; cm⁻¹): 2964, 2916, 1591, 1361, 1261, 1093, 1032, 800. Anal. Calcd for C₁₆H₁₉Br₂MoS₂: C, 36.18; H, 3.61. Found: C, 36.23; H, 3.91.

Preparation of [Cp*Ru(μ - η^2 : η^2 -bdt)(μ -Br)MoBrCp*][PF₆] (2)

[Cp*Ru(MeCN)₃][PF₆] (50.4 mg, 0.10 mmol) was added to a reddish purple solution of **1** (53.1 mg, 0.10 mmol) in 5 mL CH₂Cl₂ at room temperature, then the solution color turned to brown immediately. After stirring for 1 h, the resulting solution was evaporated to dryness under vacuum, then the residues were washed with Et₂O (3 × 3 mL). The filtrate was dried in reduced pressure to obtain a brown powder [Cp*Ru(μ - η^2 : η^2 -bdt)(μ -Br)MoBrCp*][PF₆] (**2**, 80.3 mg, 0.088 mmol, 88%). Crystals of **2** suitable for X-ray diffraction experiment were grown from saturated CH₂Cl₂ solution layered by *n*-hexane at room temperature. ¹H NMR (400 MHz, CD₂Cl₂, ppm, 298 K): δ 1.98 (br), 1.17 (br). μ_{eff} (CD₂Cl₂, Evans' method, 298 K): 1.89 μ_{B} . HRMS (ESI, *m/z*) Calcd for [**2**-PF₆]⁺, 767.8549, Found 767.8562. IR (Film; cm⁻¹): 3064, 2966, 2922, 2854, 1631, 1441, 1377, 1022, 842, 1072, 758, 557. Anal. Calcd for C₂₆H₃₄Br₂F₆MoPRuS₂: C, 34.22; H, 3.76. Found: C, 34.27; H, 3.69.

Preparation of [Cp*Ru(μ - η^4 : η^2 -bdt)MoBr₂Cp*] (**3**)

CoCp₂ (19 mg, 0.10 mmol) was added to a CH₂Cl₂ solution of **2** (91.3 mg, 0.10 mmol) with vigorously stirring at room temperature. After stirring for 12 h, the resulting solution was evaporated to dryness under vacuum and washed by 5 mL Et₂O. The filtrate was dried in reduced pressure to obtain a brown crystalline powder [Cp*Ru(μ - η^4 : η^2 -bdt)MoBr₂Cp*] (**3**, 58.4 mg, 0.076 mmol, 76%). Crystals of **2** suitable for X-ray diffraction experiment were grown from saturated CH₂Cl₂ solution layered by *n*-hexane at room temperature. ¹H NMR (400 MHz, CD₂Cl₂, ppm): δ 7.63 (dd, $J_1 = 6.5$ Hz, $J_2 = 3.2$ Hz, 2H, bdt-*H*), 7.52 (dd, $J_1 = 6.5$ Hz, $J_2 = 3.1$ Hz, 2H, bdt-*H*), 1.53 (s, 15H, Cp*-CH₃), 1.52 (s, 15H, Cp*-CH₃). IR (Film; cm⁻¹): 3047, 2960, 2918, 2856, 1437, 1375, 1261, 1099, 1024, 804, 744. Anal. Calcd for C₂₆H₃₄Br₂MoRuS₂: C, 40.69; H, 4.47. Found: C, 40.44; H, 4.28.

Preparation of [Cp*Ru(μ - η^2 : η^1 -bdt)(μ -NH₂)Mo(N)Cp*] (**4**)

Anhydrous hydrazine (25.6 mg, 0.80 mmol) was added to a solution of **3** (76.9 mg, 0.10 mmol) in THF (5 mL) and stirred at 60 °C for 6 h. After removal of the solvent under reduced pressure at room temperature, the residual solids were extracted with *n*-hexane (5 mL) and dried under vacuum. The product [Cp*Ru(μ - η^2 : η^1 -bdt)(μ -NH₂)Mo(N)Cp*] (**4**, 37.1 mg, 0.058 mmol, 58%) was obtained as a brown powder. ¹H NMR (400 MHz, CD₂Cl₂, ppm): δ 7.60 (m, 1H, bdt-*H*), 6.96 (m, 1H, bdt-*H*), 6.73 (m, 2H, bdt-*H*), 4.82 (s, 1H, NHH), 3.50 (s, 1H, NHH), 1.69 (s, 15H, Cp*-CH₃), 1.64 (s, 15H, Cp*-CH₃). IR (film, cm⁻¹): 3375(ν_{NH}), 3278(ν_{NH}), 2962, 2910, 2852, 1566, 1437, 1261, 1095, 1030, 998($\nu_{\text{Mo=N}}$), 798, 742. Anal. Calcd for C₂₆H₃₆MoN₂RuS₂: C, 48.97; H, 5.69; N, 4.39. Found: C, 49.44; H, 5.74; N, 4.15.

A sample of ¹⁵N-**4** was synthesized using an analogous synthetic procedure with ¹⁵N₂H₄ in 52% yield based on complex **3** (0.10 mmol). ¹H NMR (400 MHz, CD₂Cl₂): δ 7.59 (m, 1H, bdt-*H*), 6.97 (m, 1H, bdt-*H*), 6.73 (m, 2H, bdt-*H*), 4.83 (dd, $J_1 = 5.6$ Hz, $J_2 = 73.4$ Hz, 1H, NHH), 3.50 (dd, $J_1 = 5.8$ Hz, $J_2 = 71.1$ Hz, 1H, NHH), 1.69 (s, 15H, Cp*-CH₃), 1.63 (s, 15H, Cp*-CH₃). ¹⁵N NMR (61 MHz, CD₂Cl₂, ppm): δ 59.70 (t, $^1J_{\text{NH}} = 72.6$ Hz, 1N, NH₂), 848.67. IR (film, cm⁻¹): 3365($\nu_{15\text{NH}}$), 3267($\nu_{15\text{NH}}$),

3043, 2962, 2908, 2850, 1774, 1566, 1435, 1260, 1095, 1028, 971($\nu_{\text{Mo}=\text{15N}}$), 796, 742.

Preparation of [Cp***Ru**(μ - η^1 : η^2 -bdt)(μ -NH₂)₂MoCp*] (**5**)

NaNH₂ (7.8 mg, 0.20 mmol) was added to a THF (5 mL) solution of **3** (76.9 mg, 0.10 mmol) at room temperature. After stirring for 24 h, the mixture was evaporated to dryness under vacuum. The residual solids were extracted with *n*-hexane (5 mL). The extract was dried in reduced pressure to obtain **5** as a brown power (40.4 mg, 0.063 mmol, 63%). Crystals of **5** suitable for X-ray diffraction experiment were grown from saturated CH₂Cl₂ solution layered by *n*-hexane at room temperature. ¹H NMR (400 MHz, CD₂Cl₂, ppm, 298 K): δ 7.50 (m, 2H, bdt-*H*), 6.81 (m, 2H, bdt-*H*), 1.57 (s, 15H, Cp*-CH₃), 1.47 (s, 15H, Cp*-CH₃), -0.62 (s, 4H, NHH). IR (Film; cm⁻¹): 3359(ν_{NH}), 3317(ν_{NH}), 3047, 2974, 2898, 1648, 2852, 1566, 1435, 1377, 1026, 802, 742. Anal. Calcd for C₂₆H₃₈MoN₂RuS₂: C, 48.81; H, 5.99; N, 4.38. Found: C, 49.38; H, 5.72; N, 4.14.

Formation of **4** from **5**

^tBu₃C₆H₂O · (52.2 mg, 0.20 mmol) was added to a CH₂Cl₂ solution of **5** (64.2 mg, 0.10 mmol) with vigorously stirring at room temperature. The mixture was stirred for 6 h. Then, the resulting solution was evaporated to dryness under vacuum and extracted with *n*-hexane (5 mL). The filtrate was dried in reduced pressure to obtain **4** as a brown crystalline powder (28.8 mg, 0.045 mmol, 45%).

Typical procedure for the catalytic reduction of hydrazine

Lut HBPh₄ (170.8 mg, 0.40 mmol) and CoCp₂ (75.6 mg, 0.40 mmol) were added to a THF (5 mL) solution containing **4** (12.8 mg, 0.02 mmol) and anhydrous hydrazine (6.4 mg, 0.20 mmol) under an argon atmosphere. The mixture was stirred at room temperature for 12 h. The reaction volatiles were vacuum-transferred into a frozen diethyl ether solution of HCl (6 M, 3 mL) in a Schlenk flask. Then, excess KO^tBu in THF (10 mL) was added to the original reaction Schlenk vial and stirred for additional 30 min. The volatiles were also transferred into the Schlenk flask containing the frozen HCl solution. The vacuum-transferred products were stirred for 20 min at room temperature and then the

volatile components were removed in reduced pressure. The ^1H NMR ($\text{DMSO-}d_6$) spectrum of the remained solids showed the presence of Lut HCl and NH_4Cl as the principal components. The NH_4Cl was quantified by integration of the NH_4^+ resonance with respect to an internal reference of ferrocene (**Figure S16**).

References

1. J. U. Desai, J. C. Gordon, H.-B. Kraatz, B. E. Owens-Waltermire, R. Poli and A. L. Rheingold, *Angew. Chem. Int. Ed.*, **1993**, 32, 1486–1488.
2. H. J. Zhang, B. Demerseman, Z. Xi and C. Bruneau, *Eur. J. Inorg. Chem.*, **2008**, 20, 3212–3217.
3. E. Block, V. Eswarakrishnan, M. Gernon, G. Ofori-Okai, C. Saha, K. Tang and J. Zubieta, *J. Am. Chem. Soc.*, **1989**, 111, 658–665.
4. V. W. Manner, T. F. Markle, J. H. Freudenthal, J. P. Roth and J. M. Mayer, *Chem. Commun.*, **2008**, 2, 256–258.
5. P. A. Ulmann, A. B. Braunschweig, O. S. Lee, M. J. Wiester, G. C. Schatz and C. A. Mirkin, *Chem. Commun.*, **2009**, 34, 5121–5123.
6. T. E. Glassman, M. G. Vale and R. R. Schrock, *J. Am. Chem. Soc.*, **2002**, 114, 8098–8109.
7. G. M. Sheldrick, *Sadabs*, SADABS, Program for area detector adsorption correction, Institute for Inorganic Chemistry, University of Göttingen, Germany, 1996.
8. L. Palatinus and G. Chapuis, *J. Appl. Cryst.*, **2007**, 40, 786–790.
9. O. V. Dolomanov, L. J. Bourhis, R. J. Gildea, J. A. K. Howard and H. Puschmann, *J. Appl. Cryst.*, **2009**, 42, 339–341.

X-ray Crystallographic Information

Table S1. Crystallographic data for **1** and **2**.

	1	2
Formula	C ₁₆ H ₁₉ Br ₂ MoS ₂	C ₂₆ H ₃₄ Br ₂ F ₆ MoPRuS ₂
Formula weight	531.19	912.45
Crystal dimensions (mm ³)	0.1 × 0.1 × 0.1	0.2 × 0.2 × 0.1
Crystal system	monoclinic	orthorhombic
Space group	<i>C2/c</i>	<i>Pca2₁</i>
a (Å)	26.4098(18)	28.2657(16)
b (Å)	9.3502(6)	8.3531(5)
c (Å)	29.2033(19)	27.0412(16)
α (°)	90	90
β (°)	193.3411(0)	90
γ (°)	90	90
Volume (Å ³)	7199.1(8)	6384.6(6)
Z	16	8
T (K)	222.99	230.01
D _{calcd} (g cm ⁻³)	1.960	1.899
μ (mm ⁻¹)	5.392	3.602
F (000)	4144.0	3576.0
No. of rflns. collected	53189	38817
No. of indep. rflns. /R _{int}	6341 / 0.0272	9073 / 0.0388
No. of obsd. rflns. [<i>I</i> ₀ > 2σ(<i>I</i> ₀)]	5840	16586
Data / restraints / parameters	6341 / 0 / 380	9073 / 14 / 704
R ₁ / wR ₂ [<i>I</i> ₀ > 2σ(<i>I</i> ₀)] ^a	0.0266 / 0.0597	0.0376 / 0.0932
R ₁ / wR ₂ (all data) ^a	0.0307 / 0.0608	0.0463 / 0.0966
GOF (on F ²) ^a	1.187	1.030
Largest diff. peak and hole (e Å ⁻³)	0.57 / -0.54	0.73 / -0.71
CCDC No.	2161596	2161603

Table S2. Crystallographic data for **3** and **4**.

	3	4
Formula	C ₂₆ H ₃₄ Br ₂ MoRuS ₂	C ₂₆ H ₃₆ MoN ₂ RuS ₂
Formula weight	767.48	637.70
Crystal dimensions (mm ³)	0.3 × 0.25 × 0.2	0.3 × 0.2 × 0.2
Crystal system	monoclinic	monoclinic
Space group	<i>P</i> 2 ₁ / <i>c</i>	<i>P</i> 2 ₁ / <i>n</i>
a (Å)	8.8970(6)	13.1999(11)
b (Å)	31.824(2)	10.4937(9)
c (Å)	19.9124(14)	19.7054(16)
α (°)	90	90
β (°)	93.466(12)	92.836(2)
γ (°)	90	90
Volume (Å ³)	5627.6(7)	2726.2(4)
<i>Z</i>	8	4
<i>T</i> (K)	180.0	294.0
<i>D</i> _{calcd} (g cm ⁻³)	1.812	1.554
μ (mm ⁻¹)	3.984	1.183
<i>F</i> (000)	3024.0	1296.0
No. of rflns. collected	72992	32086
No. of indep. rflns. / <i>R</i> _{int}	9959 / 0.0490	6858 / 0.0712
No. of obsd. rflns. [<i>I</i> ₀ > 2σ(<i>I</i> ₀)]	8967	4542
Data / restraints / parameters	9959 / 0 / 578	6858 / 0 / 299
<i>R</i> ₁ / <i>wR</i> ₂ [<i>I</i> ₀ > 2σ(<i>I</i> ₀)] ^a	0.0561 / 0.1144	0.0500 / 0.0820
<i>R</i> ₁ / <i>wR</i> ₂ (all data) ^a	0.0636 / 0.1170	0.1010 / 0.0977
GOF (on <i>F</i> ²) ^a	1.261	1.034
Largest diff. peak and hole (e Å ⁻³)	2.62 / -0.85	0.89 / -0.61
CCDC No.	2161605	2161650

Table S3. Crystallographic data for **5**.

5	
Formula	C ₂₆ H ₃₈ MoN ₂ RuS ₂
Formula weight	639.71
Crystal dimensions (mm ³)	0.1 × 0.1 × 0.1
Crystal system	orthorhombic
Space group	<i>Pbca</i>
a (Å)	14.8725(14)
b (Å)	16.2572(16)
c (Å)	22.557(2)
α (°)	90
β (°)	90
γ (°)	90
Volume (Å ³)	5454.0(9)
Z	8
T (K)	297.0
D _{calcd} (g cm ⁻³)	1.558
μ (mm ⁻¹)	1.183
F (000)	2608.0
No. of rflns. collected	35336
No. of indep. rflns. /R _{int}	5575 / 0.0604
No. of obsd. rflns. [I ₀ > 2σ(I ₀)]	4132
Data / restraints / parameters	5575 / 1 / 299
R ₁ / wR ₂ [I ₀ > 2σ(I ₀)] ^a	0.0596 / 0.1462
R ₁ / wR ₂ (all data) ^a	0.0870 / 0.1662
GOF (on F ²) ^a	1.049
Largest diff. peak and hole (e Å ⁻³)	2.83 / -0.98
CCDC No.	2161653

Figure S1. ORTEP diagram of **1**, hydrogen atoms are omitted for clarity (thermal ellipsoids shown at 50% probability).

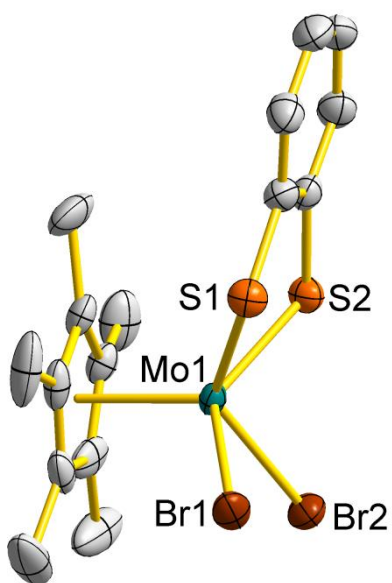


Table S4. Selected bond distances (Å) and bond angles (°) for **1**.

Distances (Å)			
Mo1–S1	2.3626(12)	Mo1–S2	2.3482(12)
Mo1–Br1	2.5334(6)	Mo1–Br2	2.5325(6)
Angles (°)			
S1–Mo1–S2	81.27(4)	Br1–Mo1–Br2	85.89(2)

Figure S2. ORTEP diagram of **2**, counter anion PF_6^- and hydrogen atoms on carbons are omitted for clarity (thermal ellipsoids shown at 50% probability).

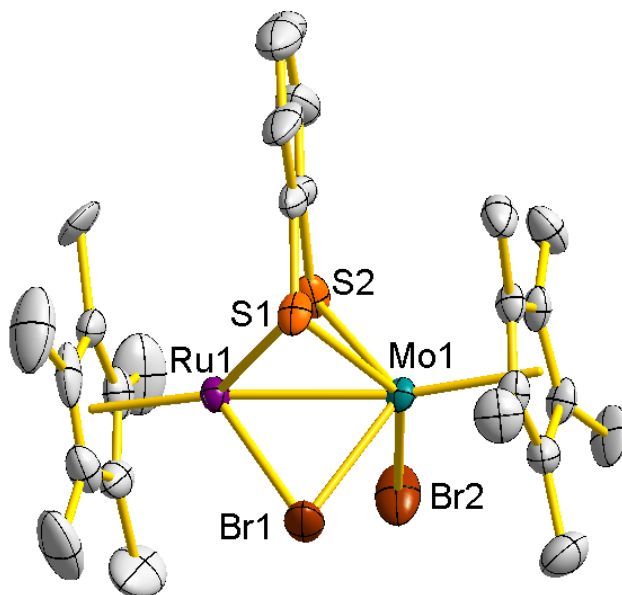


Table S5. Selected bond distances (Å), angles (°) and torsion angles (°) for **2**.

Distances (Å)			
Mo1–Ru1	2.6954(2)	Mo1–S1	2.5039(1)
Mo1–S2	2.3858(1)	Mo1–Br1	2.5341(1)
Mo1–Br2	2.5583(1)	Ru1–S1	2.4093(1)
Ru1–S2	2.3377(1)	Ru1–Br1	2.5278(1)
Angles (°)			
Mo1–S1–Ru1	66.509(3)	Mo1–S2–Ru1	69.580(3)
S1–Mo1–S2	75.124(3)	S1–Ru1–S2	77.825(4)
Mo1–Br1–Ru1	64.348(3)		
Torsion angles (°)			
S1–Mo1Ru1–S2	96.624(4)	Ru1–S1S2–Mo1	90.863(4)

Figure S3. ORTEP diagram of **3**, hydrogen atoms on carbons are omitted for clarity (thermal ellipsoids shown at 50% probability).

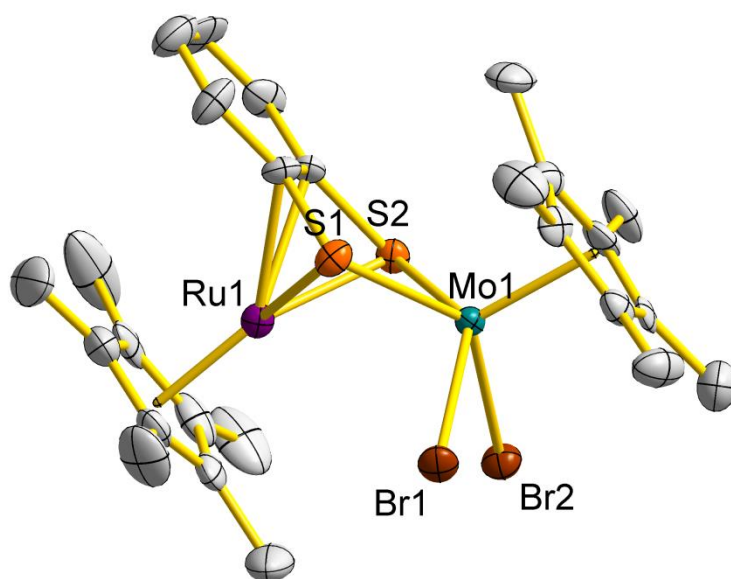


Table S6. Selected bond distances (Å), angles (°) and torsion angles (°) for **3**.

Distances (Å)			
Mo1··Ru1	3.0241(2)	Mo1-S1	2.3556(1)
Mo1-S2	2.3504(2)	Mo1-Br1	2.6174(1)
Mo1-Br2	2.5999(2)	Ru1-S1	2.3457(1)
Ru1-S2	2.3391(1)		
Angles (°)			
Mo1-S1-Ru1	80.071(3)	Mo1-S2-Ru1	80.311(3)
S1-Mo1-S2	83.563(2)	S1-Ru1-S2	84.028(3)
Torsion angles (°)			
S1-Mo1Ru1-S2	121.614(4)	Ru1-S1S2-Mo1	119.831(4)

Figure S4. ORTEP diagram of **4**, hydrogen atoms except for the bridging NH₂ group are omitted for clarity (thermal ellipsoids shown at 50% probability).

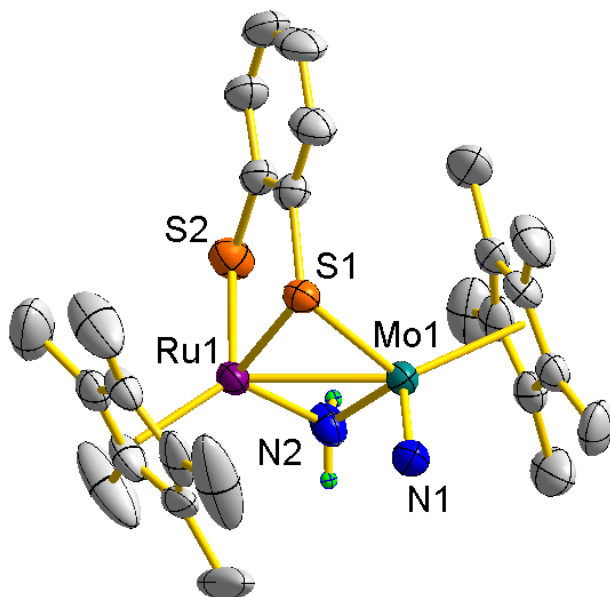


Table S7. Selected bond distances (Å), angles (°) and torsion angles (°) for **4**.

Distances (Å)			
Mo1–Ru1	2.7277(2)	Mo1–N1	1.6609(1)
Mo1–N2	2.0736(1)	Ru1–N2	2.0872(1)
Mo1–S1	2.4122(1)	Ru1–S1	2.2992(1)
Ru1–S2	2.3774(1)		
Angles (°)			
Mo1–N2–Ru1	81.925(3)	Mo1–S1–Ru1	70.710(2)
S1–Ru1–S2	86.612(2)		
Torsion angles (°)			
S1–Mo1Ru1–N2	165.046(3)	Mo1–S1Ru1–S2	97.450(2)

Figure S5. ORTEP diagram of **5**, hydrogen atoms except for the two bridging NH₂ groups are omitted for clarity (thermal ellipsoids shown at 50% probability).

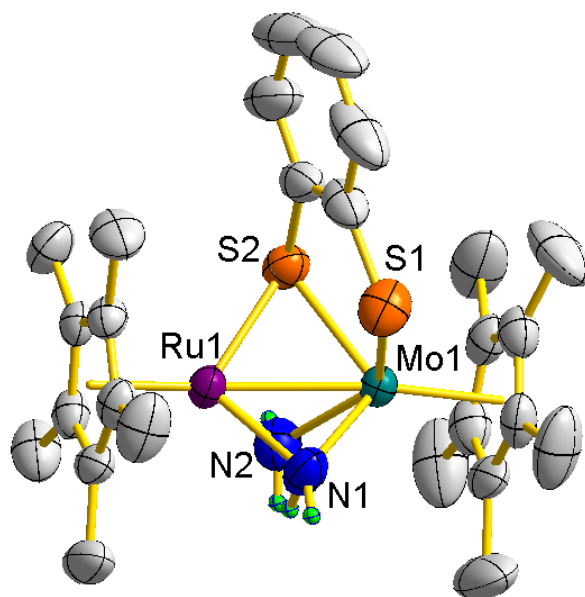


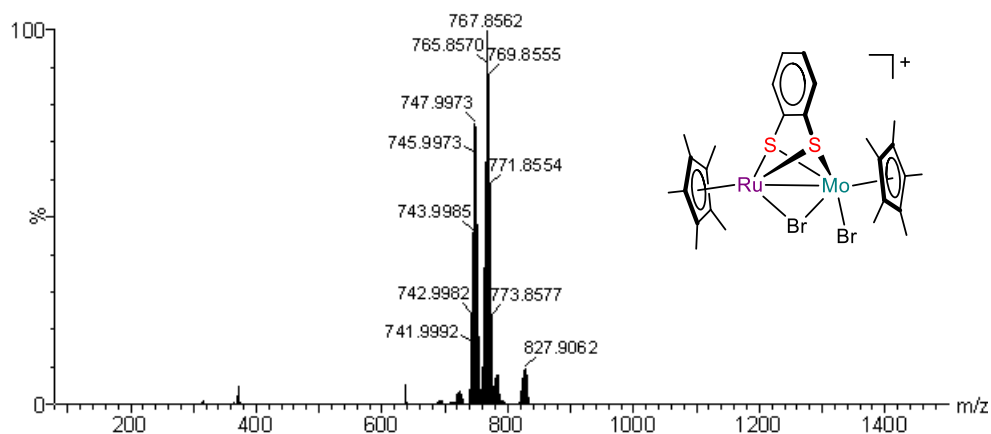
Table S8. Selected bond distances (Å), angles (°) and torsion angles (°) for **5**.

Distances (Å)			
Mo1–Fe1	2.6485(2)	Mo1–S1	2.4643(1)
Mo1–S2	2.3700(2)	Mo1–N1	2.0838(2)
Mo1–N2	2.1493(2)	Ru1–S2	2.3949(1)
Ru1–N1	2.1253(1)	Ru1–N2	2.1356(1)
Angles (°)			
Mo1–S2–Ru1	67.543(3)	Mo1–N1–Ru1	77.980(3)
Mo1–N2–Ru1	76.353(3)	S1–Mo1–S2	81.872(3)
Torsion angles (°)			
S2–Mo1Ru1–N1	165.035(4)	S2–Mo1Ru1–N2	98.366(3)
S1–Mo1Ru1–S2	88.733(3)	N1–Mo1Ru1–N2	96.599(4)

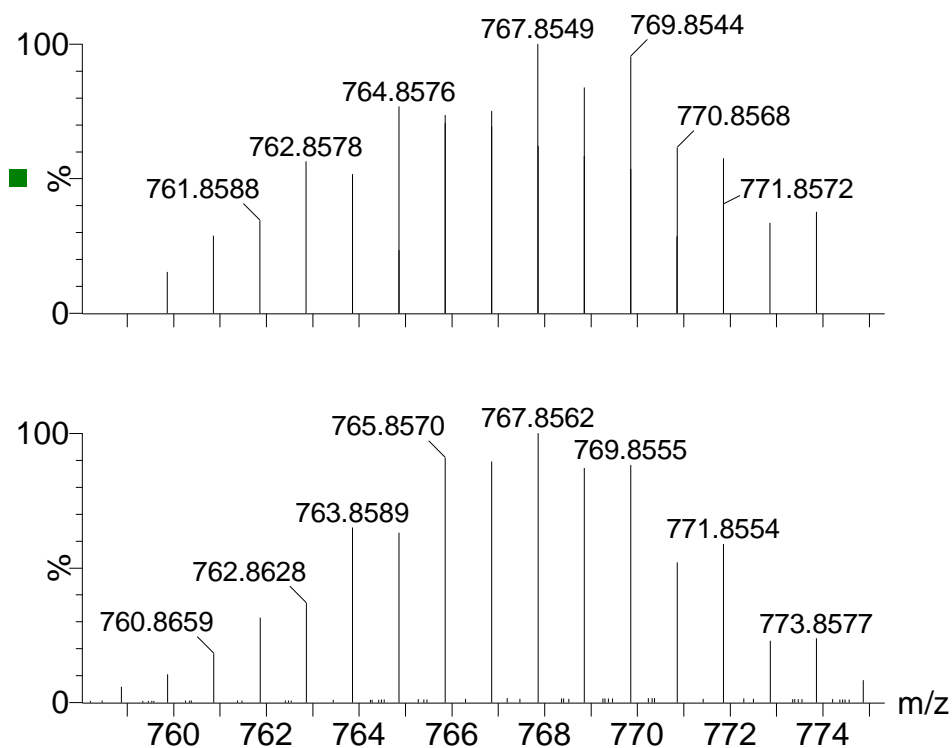
ESI High Resolution Mass Spectra

Figure S6. High resolution mass spectrum of **2** in CH₂Cl₂. (a) The signal at *m/z* 767.8562 corresponds to [2-PF₆]⁺. (b) Calculated isotopic distribution for [2-PF₆]⁺ (upper) and the amplifying experimental diagram for [2-PF₆]⁺ (bottom).

(a)



(b)



NMR Spectra

Figure S7. The ^1H NMR spectrum of **1** in CD_2Cl_2 .

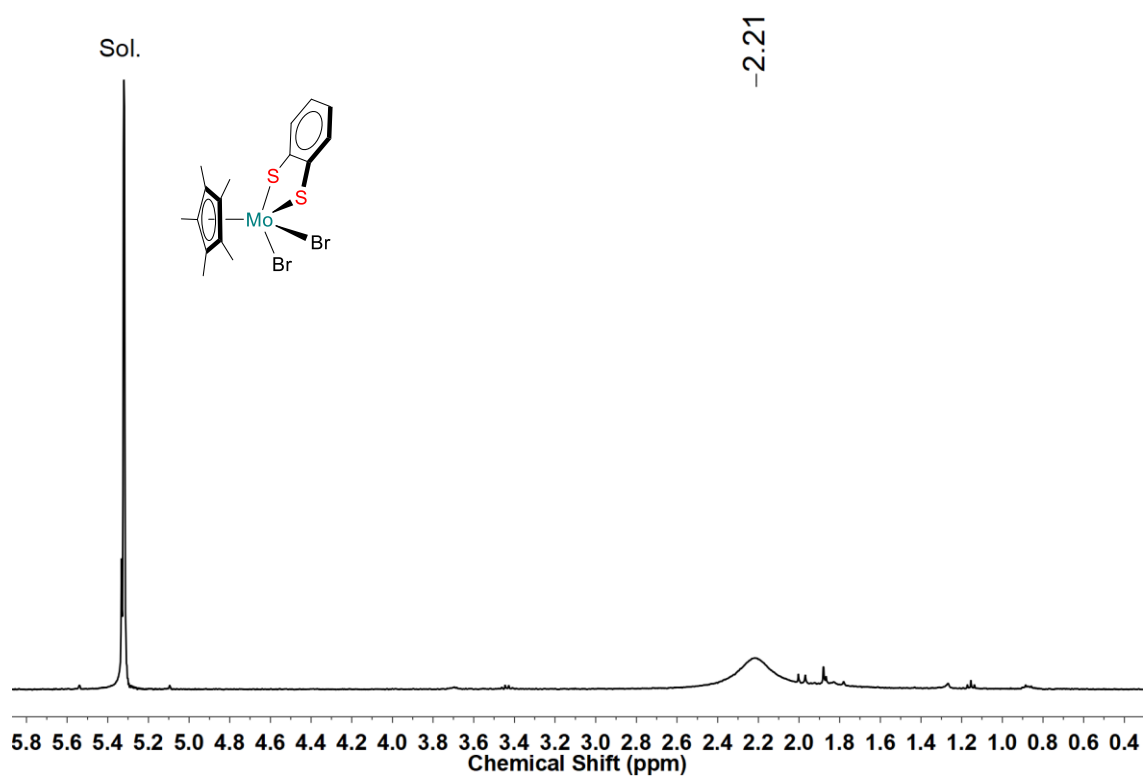


Figure S8. The ^1H NMR spectrum of **2** in CD_2Cl_2 .

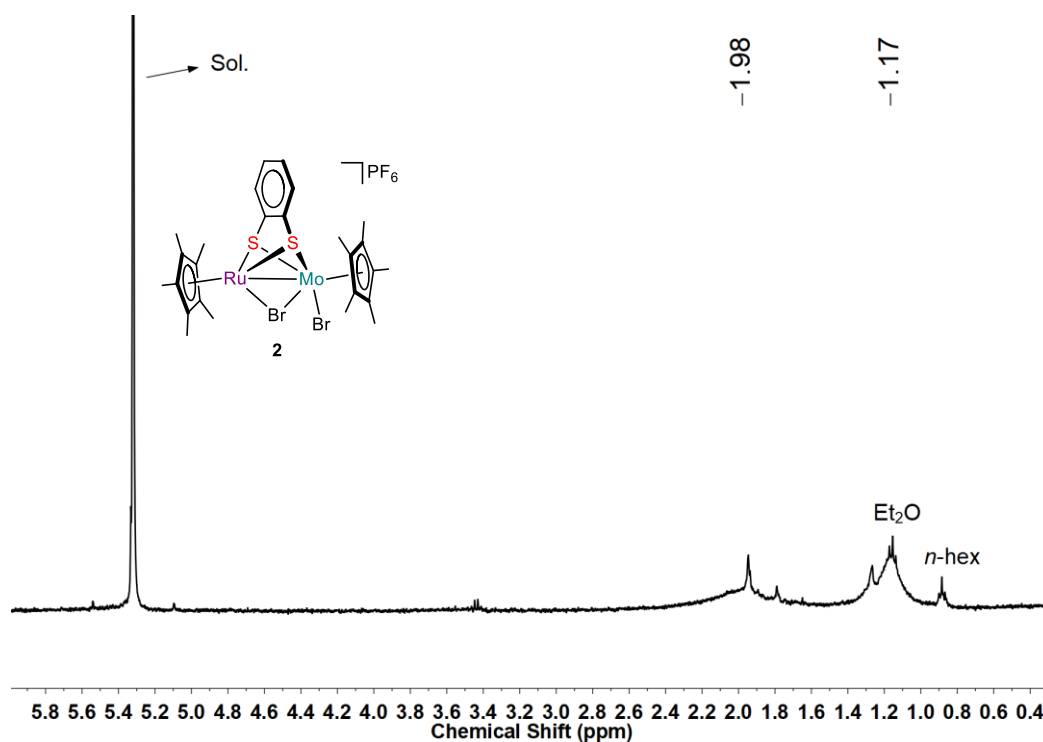


Figure S9. The ^1H NMR spectrum of **3** in CD_2Cl_2 .

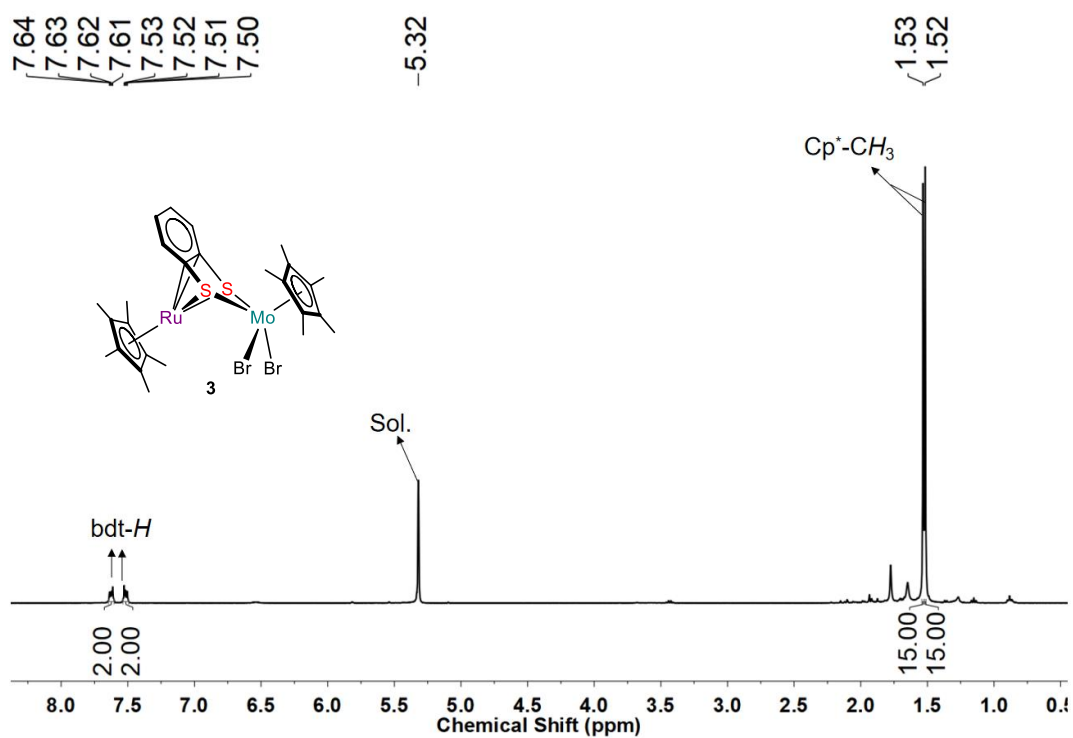


Figure S10. The ^1H NMR spectrum of **4** in CD_2Cl_2 .

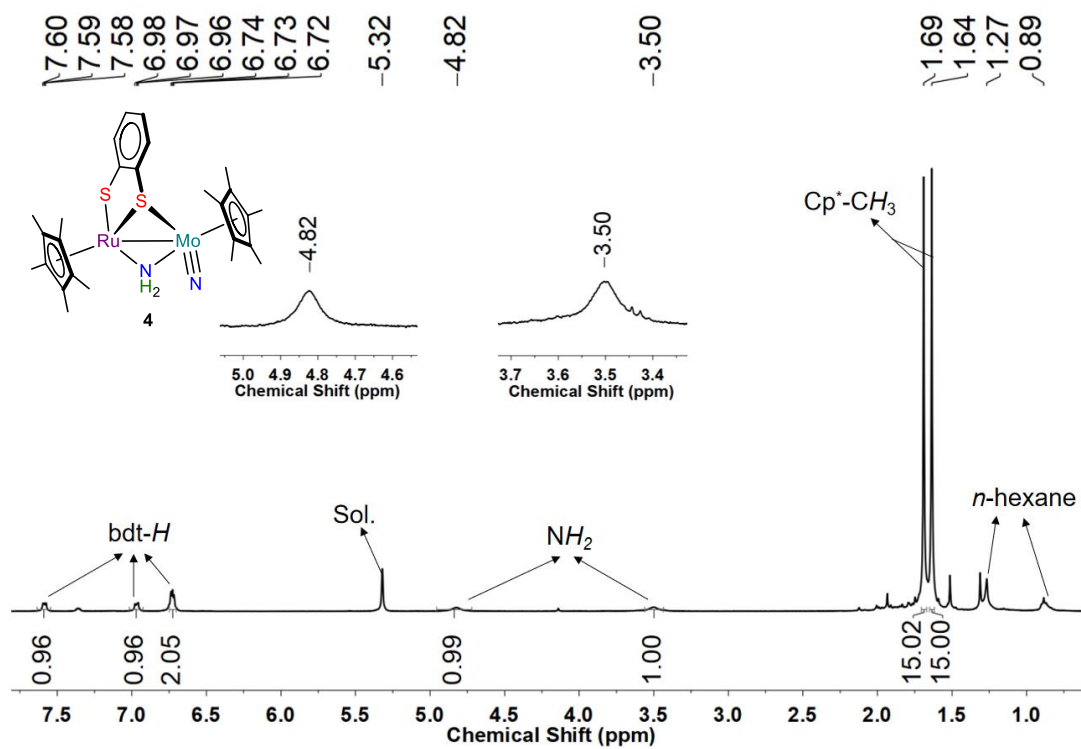


Figure S11. The ^1H NMR spectrum of ^{15}N -**4** in CD_2Cl_2

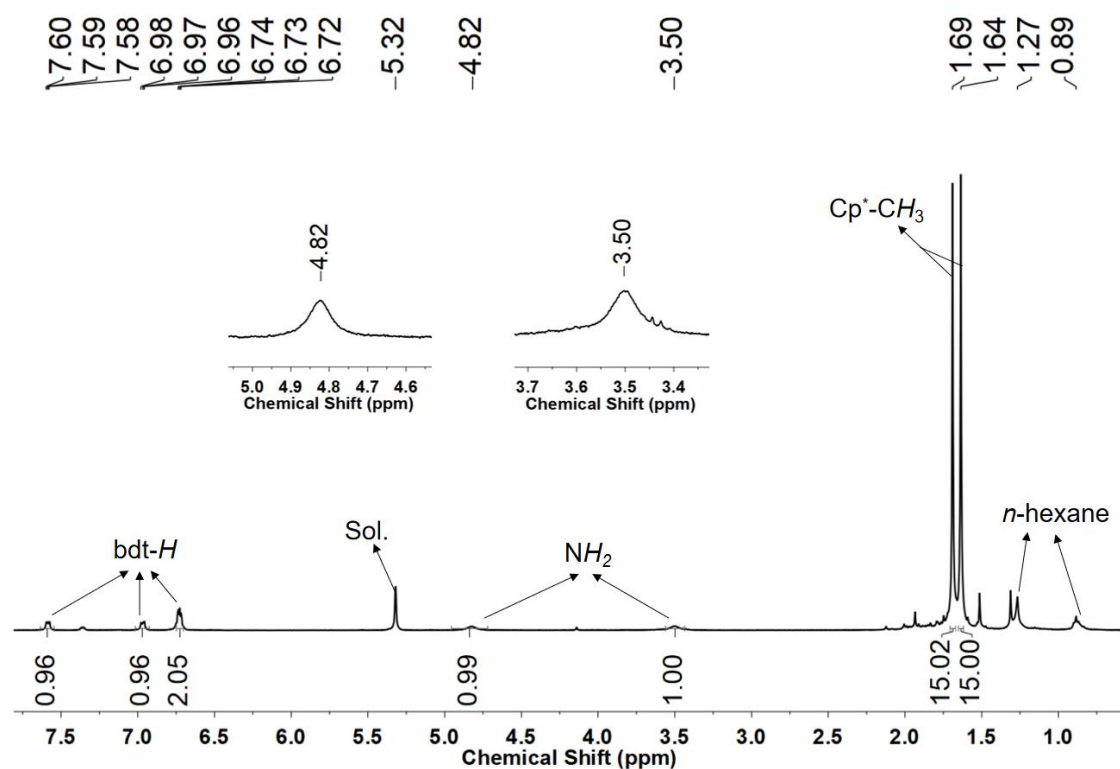


Figure S12. The $^{15}\text{N}\{^1\text{H}\}$ NMR spectrum of ^{15}N -**4** in CD_2Cl_2 .

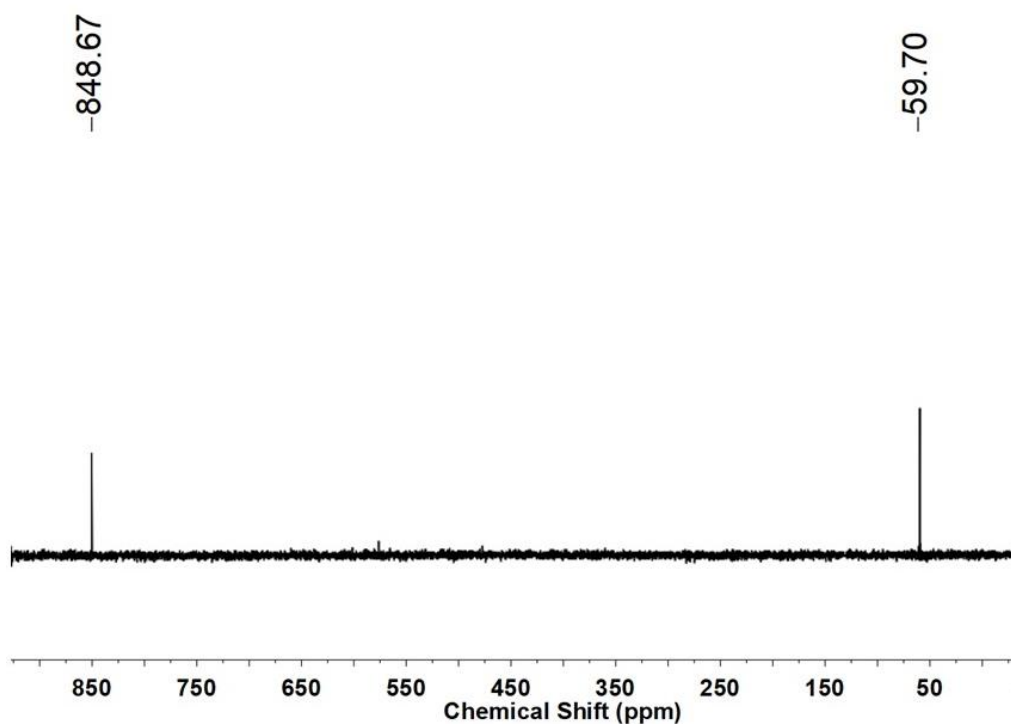


Figure S13. The ^{15}N NMR spectrum of ^{15}N -**4** in CD_2Cl_2 .

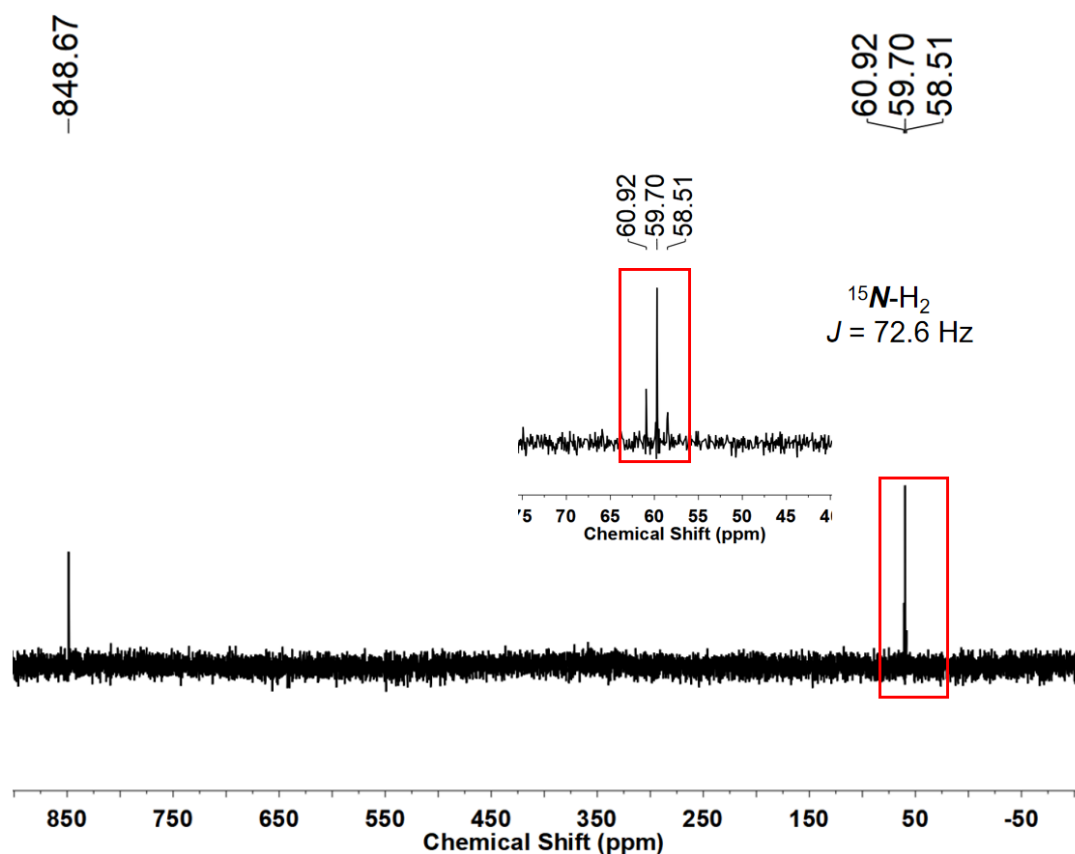


Figure S14. The ^1H NMR spectrum of **5** in CD_2Cl_2 .

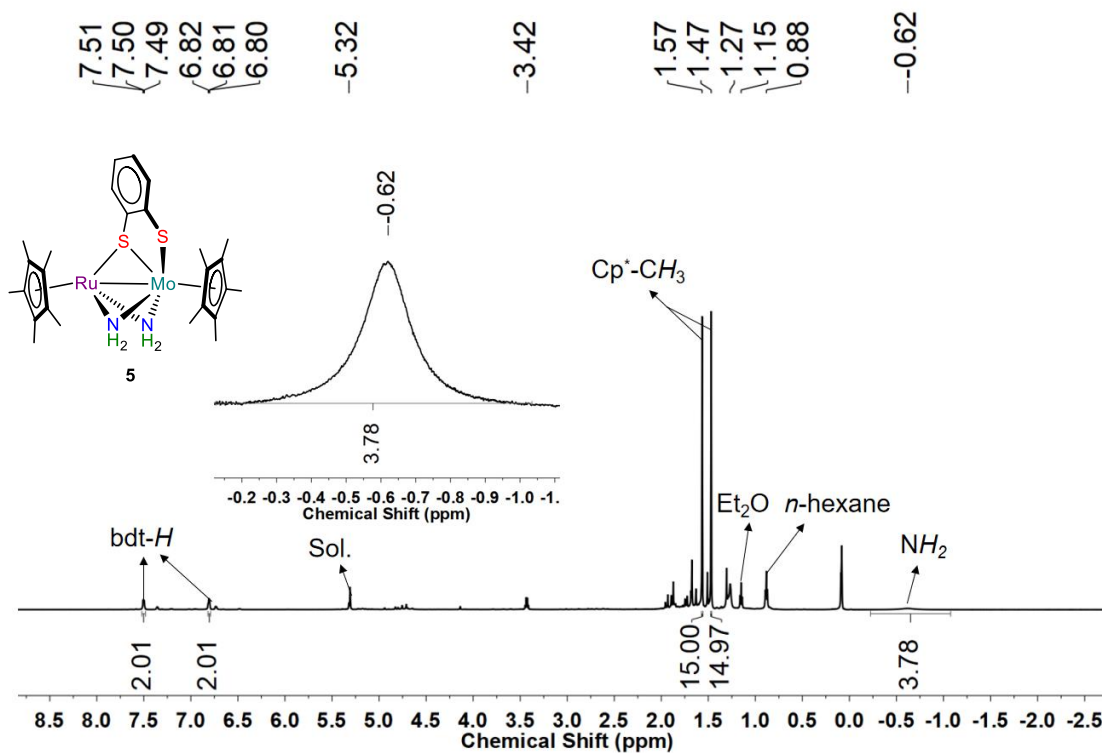


Figure S15. The ^1H NMR spectrum of the final product for reaction of complex **5** and $t\text{Bu}_3\text{C}_6\text{H}_2\text{O}$:

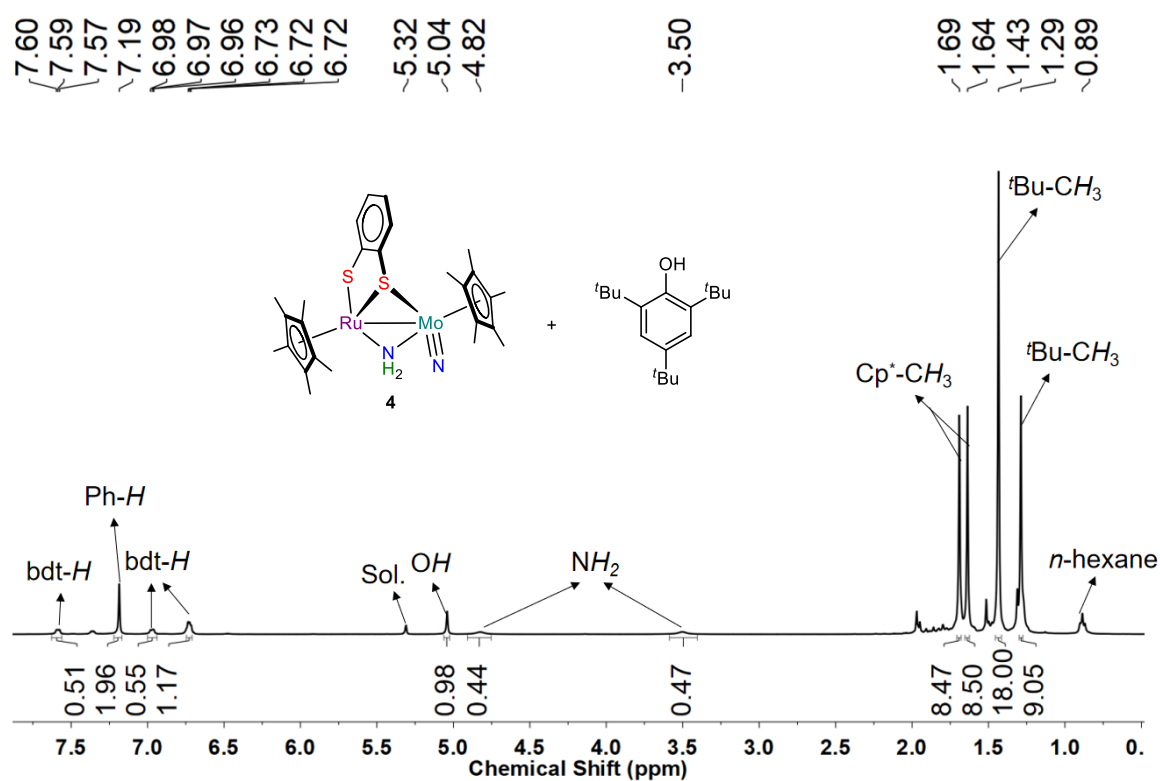
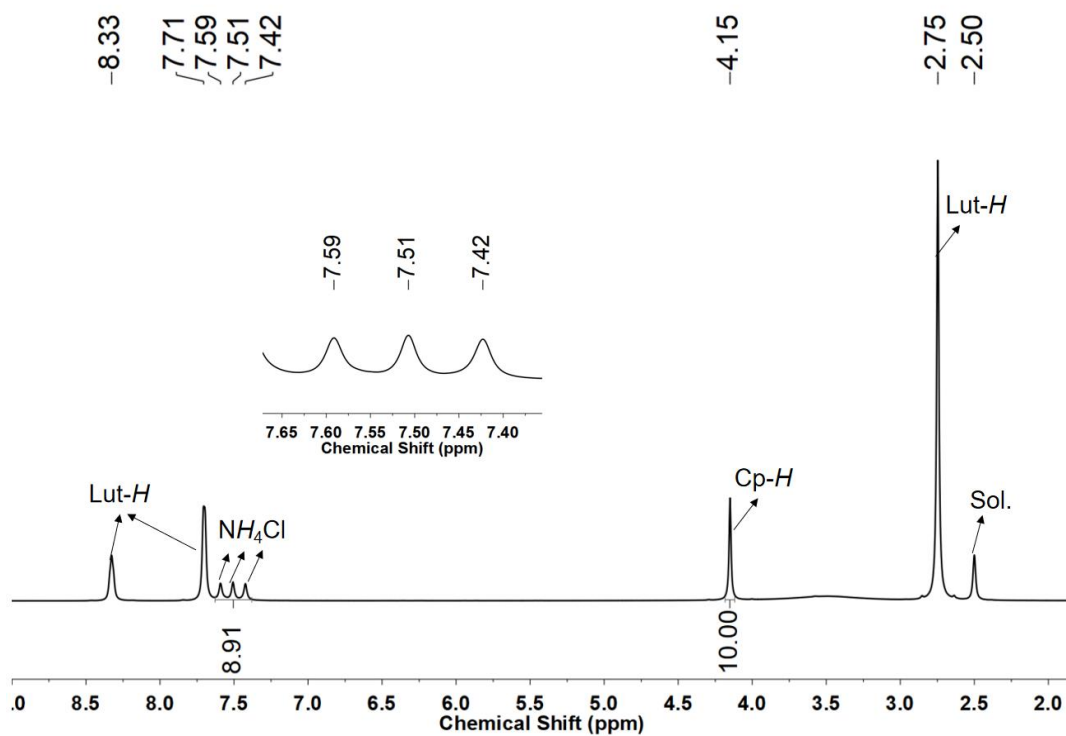


Figure S16. The ^1H NMR spectrum of NH_4Cl , FeCp_2 and $[\text{LutH}][\text{BPh}_4]$ in $\text{DMSO}-d_6$.



IR Spectra

Figure S17. The IR (film) spectrum of **1**.

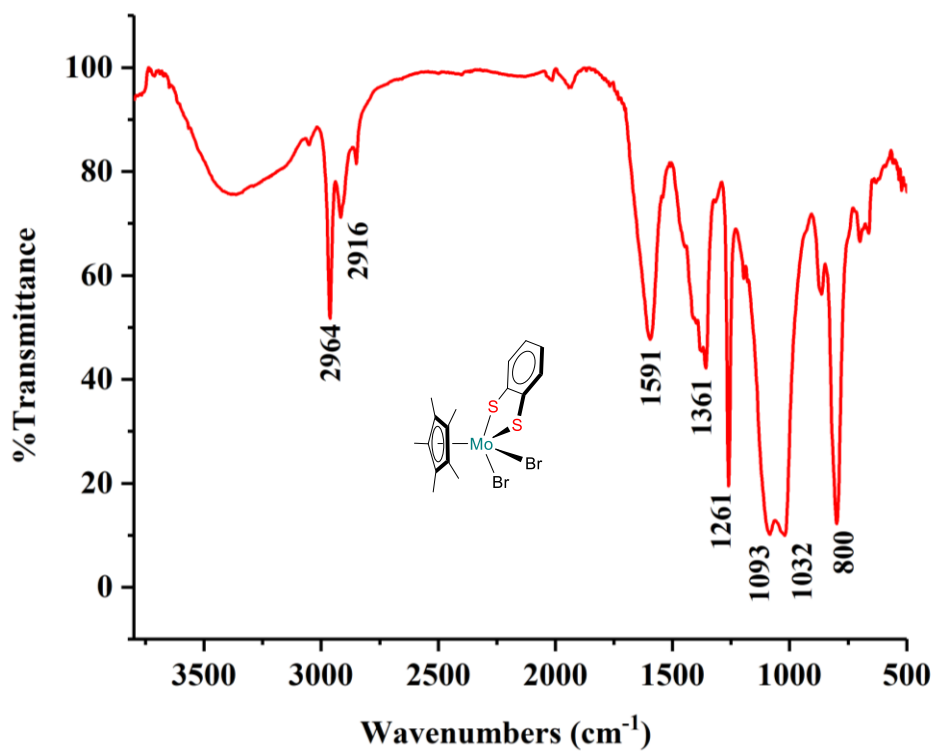


Figure S18. The IR (film) spectrum of **2**.

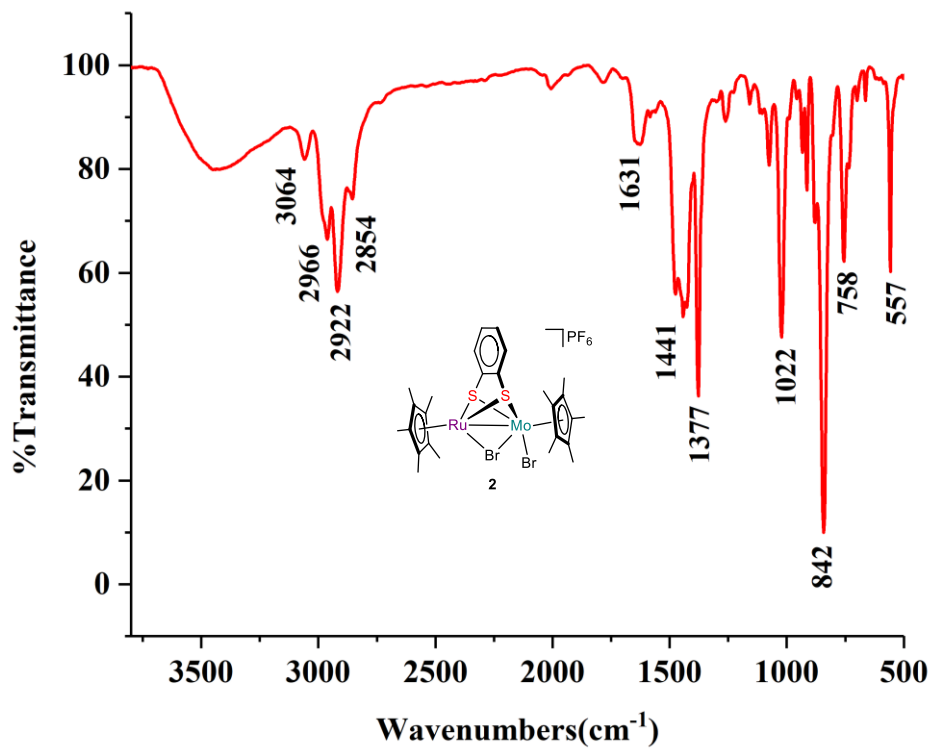


Figure S19. The IR (film) spectrum of **3**.

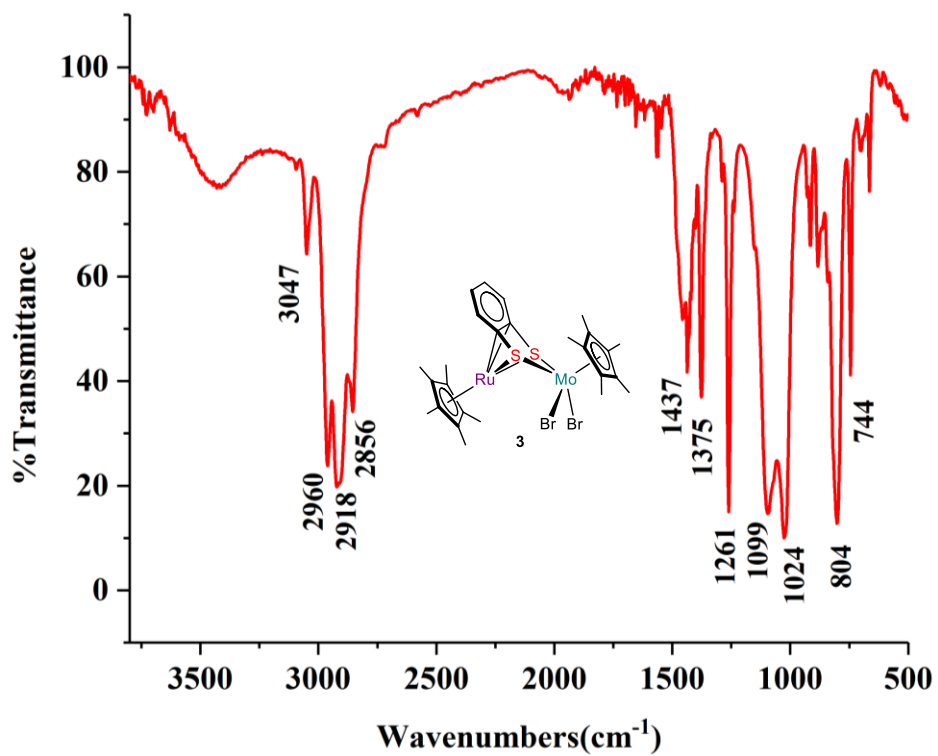


Figure S20. The IR (film) spectrum of **4**.

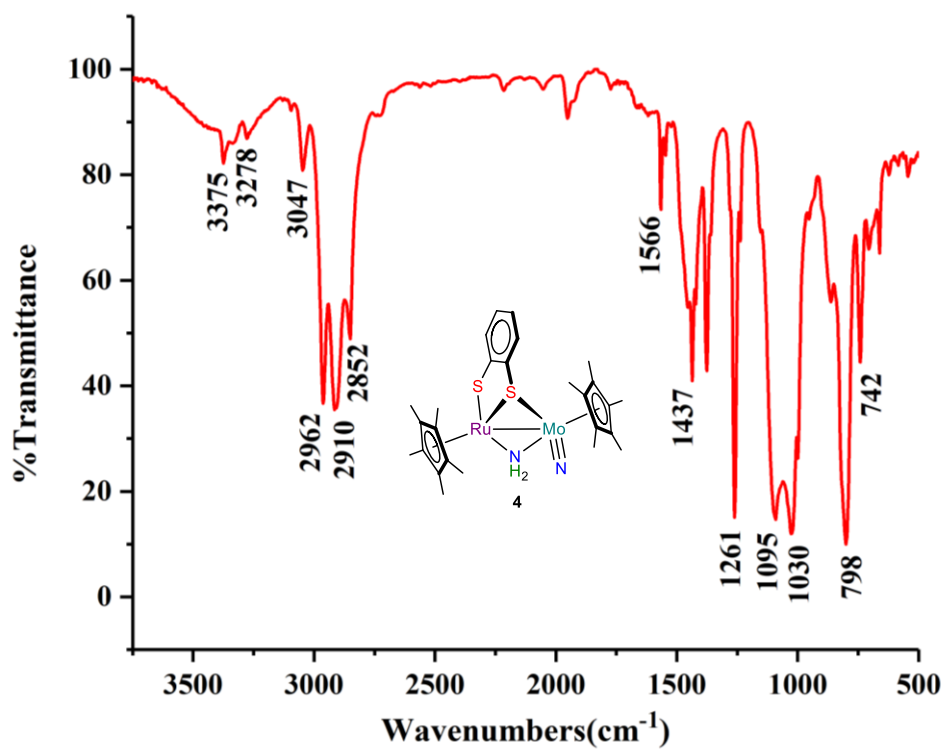


Figure S21. The IR (film) spectrum of $^{15}\text{N-4}$.

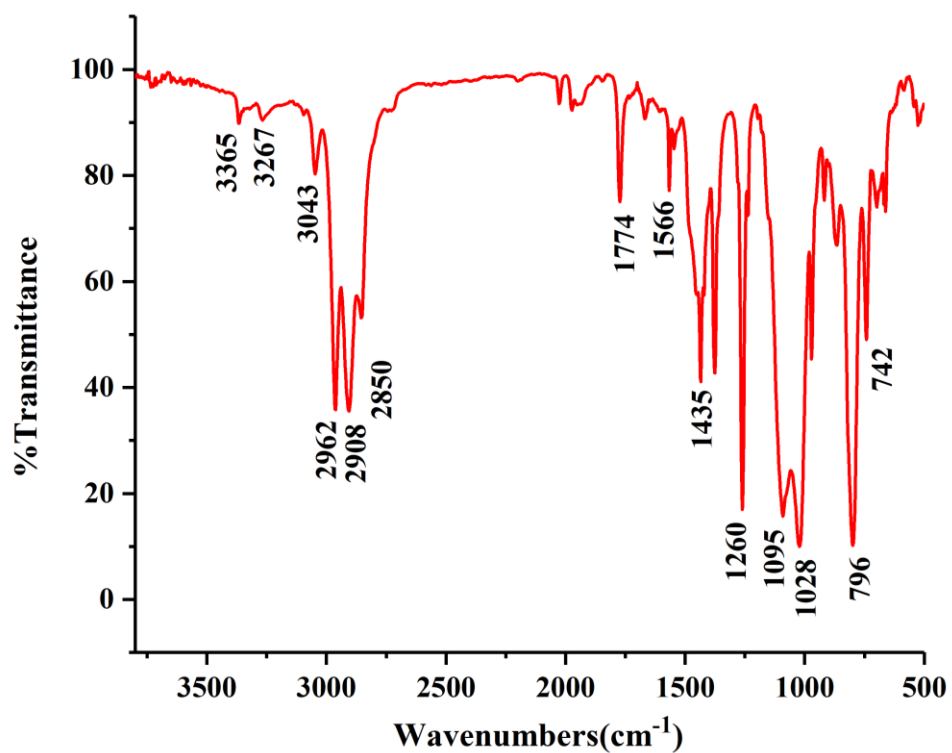


Figure S22. IR spectra of complexes **4** (blue) and $^{15}\text{N-4}$ (red), and the $^{14}\text{N-}^{15}\text{N}$ difference spectrum (green).

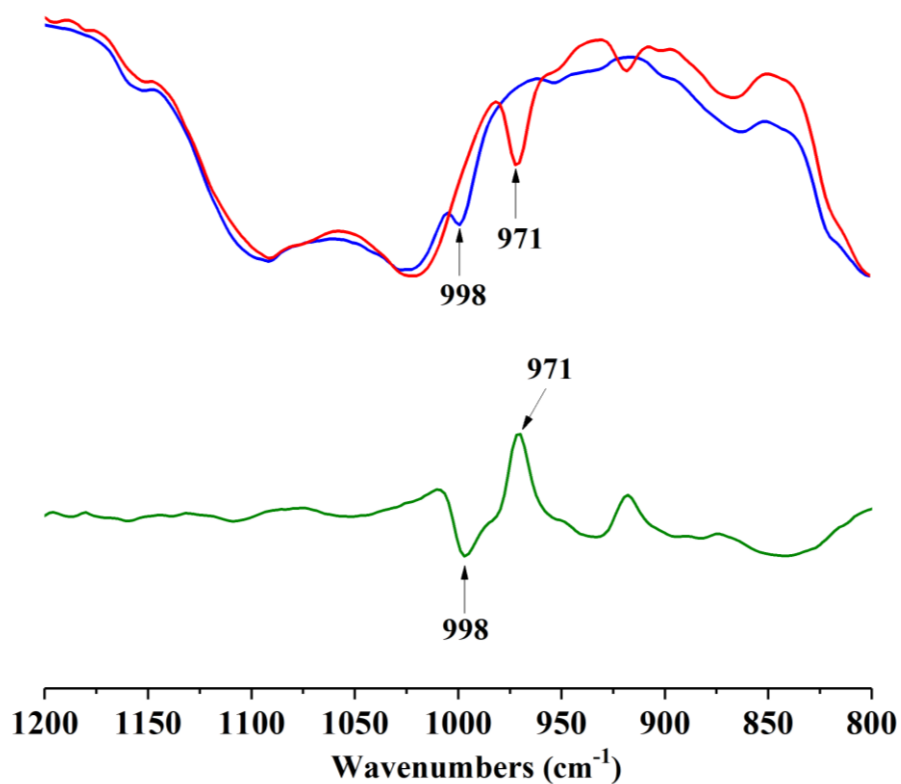


Figure S23. The IR (film) spectrum of **5**.

